Proc. of the European Safety and Reliability Conference (ESREL 2026)
Edited by José C. Matos, Paulo B. Lourenço, Michael Beer, Daniel Oliveira, Edoardo Patelli, Hélder S. Sousa, Rui A. Silva and Monica Santamaria

doi: 10.3850/ESREL2026061419_esrel26-p27691-cd

Earthquake and deterioration inclusive probabilistic life-cycle assessment (EDP-LCA) framework for existing unreinforced masonry buildings.

Daniel Caicedo

University of Minho, ISISE, ARISE, Department of Civil Engineering, Guimarães, Portugal. E-mail: dcaicedod@civil.uminho.pt

Shaghayegh Karimzadeh

University of Minho, ISISE, ARISE, Department of Civil Engineering, Guimarães, Portugal. E-mail: shaghkn@civil.uminho.pt

Paulo B. Lourenço

University of Minho, ISISE, ARISE, Department of Civil Engineering, Guimarães, Portugal. E-mail: pbl@civil.uminho.pt

This study proposes an earthquake and deterioration inclusive probabilistic life-cycle assessment (EDP-LCA) framework for existing unreinforced masonry (URM) buildings, explicitly accounting for seismic aging and material deterioration throughout the building's service life. The framework integrates robust earthquake selection based on the building exposure, nonlinear time-history analyses, and deterioration-dependent mechanical properties. A detailed macroelement model of a representative URM building is developed in OpenSees to capture variations in stiffness, strength, and energy dissipation capacity due to material degradation. The framework estimates the life-cycle embodied emissions and the additional environmental impacts associated with repair interventions triggered by recurrent seismic events. A Monte Carlo simulation is employed to account for uncertainties related to material properties, seismic hazard, and deterioration. The study highlights that the gradual loss of mechanical properties and the resulting increase in structural fragility over time significantly affect the expected environmental impact, resilience, and remaining life of existing masonry structures. The results of this research aim to support performance-based maintenance and retrofit strategies that balance structural safety and sustainability in the long-term management of existing seismic vulnerable building stock.

Keywords: Life-cycle assessment (LCA), Unreinforced masonry (URM), Seismic deterioration, Monte Carlo simulation, Performance-based maintenance.

1. Introduction

Unreinforced masonry (URM) buildings constitute a large portion of the European built heritage (Como, 2015)(Como, 2015). These structures are highly vulnerable to seismic damage mainly due to structural deterioration and exposure in regions with medium to major seismic hazard levels (Danciu et al., 2021)(Danciu et al., 2021). The structural damage caused by natural hazards can lead to significant social and economic losses together with major environmental effects. In this regard, the whole building life cycle assessment (wbLCA) approach aims to quantify the environmental impact associated with key life-cycle stages (i.e., materials production, extraction and transportation, building construction, use, and end-of-life) (Li et al., 2024)(Li et al., 2024). Nevertheless, the environmental impacts associated with building damage related to seismic events and the effect of structural deterioration are often overlooked.

In recent years, earthquake events have been recognized as a major driver of life cycle impacts rather than just a safety issue, as damage, repair, downtime, and replacement can significantly influence the environmental, economic, and social performance of buildings. In this context, concepts from performance-based earthquake engineering (PBEE) (Porter, 2003)(Porter, 2003) have been integrated with life-cycle assessment (LCA) to explicitly account for uncertainties in

seismic hazard, structural response, and post-earthquake repair actions. Several studies have laid the methodological foundation for this integration by extending conventional LCA frameworks to include earthquake-induced damage, repair processes, and probabilistic hazard scenarios (Wei et al., 2016; Belleri et al., 2016; Chhabra et al., 2018; Huang et al., 2020)(Wei et al., 2016; Belleri et al., 2016; Chhabra et al., 2018; Huang et al., 2020). In parallel, other contributions have demonstrated that seismic resilience, expressed in terms of repair time, functionality, and collapse prevention, and sustainability metrics such as carbon emissions, energy consumption, and resource use are inherently associated and should be accounted for simultaneously (Hashemi et al., 2019; Anwar et al., 2020; Welsh-Huggins et al., 2020)(Hashemi et al., 2019; Anwar et al., 2020; Welsh-Huggins et al., 2020). Ultimately, the integration of these concepts enables more effective decision-making for design and retrofit strategies, supporting balanced solutions that simultaneously address seismic safety, environmental impacts, and long-term building performance (Caruso et al., 2021; Nouri et al., 2022)(Caruso et al., 2021; Nouri et al., 2022).
This study introduces an earthquake and deterioration probabilistic (EDP)-LCA framework for existing URM buildings that explicitly accounts for both earthquake effects and time-dependent material deterioration throughout the building service life. An uncertainty propagation analysis based on Latin Hypercube Sampling (LHS) is adopted to propagate uncertainties associated with material, modelling parameters, and seismic hazard. The framework integrates hazard-consistent earthquake selection, nonlinear time-history analyses, and deterioration-dependent mechanical properties to capture the evolving structural response over time. Although preliminary, the results demonstrate that the progressive degradation of mechanical properties leads to a significant increase in structural fragility, influencing expected environmental impacts, seismic resilience, and the remaining service life of existing masonry structures. The proposed approach quantifies life-cycle embodied emissions as well as the additional environmental burdens associated with repair interventions triggered by recurrent seismic events. Overall, the framework provides strong basis to support performance-based maintenance and retrofit strategies that balance structural safety and sustainability in the long-term management of seismically vulnerable building stocks.

2. Case study definition

A representative typology of URM constructions is adopted from a portfolio of pre-code buildings in Lisbon (Bernardo et al., 2022)(Bernardo et al., 2022). The building archetype has plan dimensions of 12.50 m × 12.50 m and 3 stories with height of 3.00 m each. The load-bearing masonry walls have thicknesses of 45 cm along the main façade direction and 30 cm in the orthogonal direction. The floor system consists of timber sheathing and joists oriented perpendicular to the façades. The adopted building typology is shown in Fig. 1.

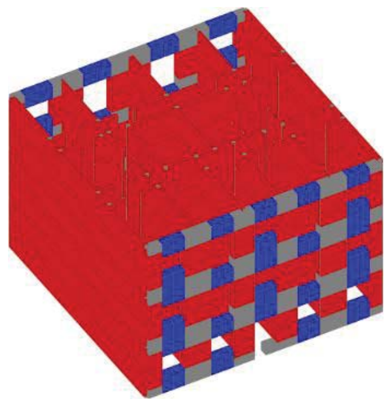

Fig. 1. URM building archetype.

2.1. *Modelling strategy*

The equivalent frame method (EFM) (D'Altri et al., 2020)(D'Altri et al., 2020) is adopted to model the building archetype in OpenSees (McKenna, 2011)(McKenna, 2011) using the macroelement formulation proposed by Vanin et al. (2020)Vanin et al. (2020). The macroelement can capture in-plane (IP) and out-of-plane (OOP) response of masonry walls. Geometric nonlinearity is accounted for through a P–Δ formulation considered in the compatibility equations to represent second-order effects. Drift demands are evaluated separately for flexural and shear deformations at the central node, with the exceedance of the corresponding thresholds leading to lateral strength degradation. The timber floors are modelled as deformable orthotropic elastic membranes, characterized by higher stiffness along the beam span. Floor-to-wall connections are represented through zero-length nonlinear interfaces to capture frictional contact and possible relative displacements that may lead to OOP collapse.

2.2. *Material and Modelling Parameters*

The LHS is adopted to ensure an efficient stratification of the multidimensional input space (Stein, 1987)(Stein, 1987). The material properties, (i.e., modulus of elasticity, E_m; shear modulus, G_m; compressive strength, f'_{cm}; cohesion, c_m; and friction coefficient, μ_m) correspond to good-quality masonry, such as regular stone or brick masonry with cement–lime mortar (Bernardo et al., 2022)(Bernardo et al., 2022). The floor stiffness factor (k_{floor}) multiplies the default stiffness values of the flexible diaphragms while the floor-to-wall friction coefficient (μ_{f-w}) defines the quality of frictional floor-wall connection (Simões, 2018; Simões et al., 2020; Almeida et al., 2020)(Simões, 2018; Simões et al., 2020; Almeida et al., 2020). The drift capacities in flexure and shear, $\delta_{c,flexure}$ and $\delta_{c,shear}$, are the limit collapse drifts at which the lateral strength of the macroelement reduces to zero (Vanin et al., 2017)(Vanin et al., 2017). An equivalent viscous damping ratio of 3%, accurate in the context of incremental dynamic analyses (IDAs) with highly non-linear structural response (Vanin et al., 2020b; Tomić et al., 2021)(Vanin et al., 2020b; Tomić et al., 2021). Fig. 2 shows the probability distributions, median values (or mean for normal distribution), and coefficients of variation (COV) adopted for the sampling of each parameter.

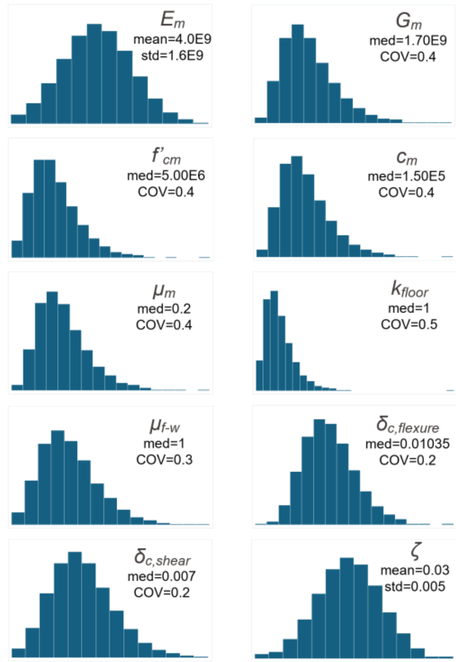

Fig. 2. Material and modelling parameters' sampling.

2.3. *Seismic action modelling*

Multiple-record IDAs are performed to explicitly capture the inherent variability of earthquake ground motions (Vamvatsikos et al., 2002)(Vamvatsikos et al., 2002). The selected seismic inputs must adequately reflect the key seismological parameters governing the distribution of intensity measures (IMs), such as moment magnitude (M_w), distance metrics (e.g., Joyner–Boore distance, R_{JB}), and site conditions (e.g., V_{S30}). The scenario-based selection criteria are defined as follows: $M_w \geq 5.5$, $R_{JB} \geq 15$ km, focal depth ≤ 70 km, and exclusion of pulse-like records. Fig. 3 presents the geometric-mean response spectra (RS) of the selected suite of 21 ground motion records.

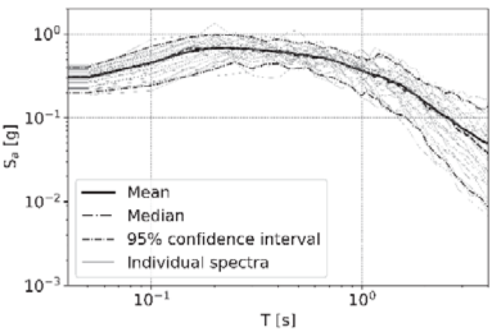

Fig. 3. RS of the selected suite of ground motions.

3. Methodology

This study proposes a surrogate-based probabilistic framework to assess the environmental consequences of seismic-induced collapse in deteriorated unreinforced masonry (URM) buildings. The methodology integrates nonlinear dynamic analysis results, surrogate modelling, deterioration staging, fragility assessment, and life-cycle environmental impact quantification.

3.1. *Surrogate modelling of seismic response*

A surrogate modelling strategy based on a Histogram Gradient Boosting Tree (HGBT) regressor is adopted to efficiently represent the seismic response of the building under uncertainty. For each LHS realisation (See Fig. 2), nonlinear dynamic analyses are conducted using the suite of ground motions reported in Section 2.3, scaled to multiple intensity levels. The maximum inter-storey drift ratio (MIDR) is selected as the engineering demand parameter (EDP) governing collapse. The predictive accuracy of the surrogate model was evaluated against the original nonlinear dynamic analyses using a *k*-fold cross-validation strategy. The validation was performed in terms of the coefficient of determination, root-mean-square error, and mean absolute error. The model achieved an average coefficient of determination of approximately $R^2 = 0.93$, indicating that the HGBT surrogate accurately reproduces the nonlinear seismic response over the range of intensities and uncertain parameters considered.

3.2. *Definition of deterioration stages*

To explicitly represent the effect of structural aging and degradation, the uncertain input parameters are grouped into four discrete deterioration stages, denoted as Stage 1 (least deteriorated) through Stage 4 (most deteriorated). In the absence of a physically calibrated time-dependent deterioration law for the investigated building, these stages are defined through a scenario-based approach. For each mechanical and modelling parameter, the empirical distribution obtained from the sampling space is divided into four bins of equal probability, representing progressively worsening material and structural conditions.

Deterioration is modelled through a monotonic reduction of stiffness, strength, and deformation capacity parameters as the stage increases. An exception is made for the damping ratio, which is assumed to increase with deterioration severity, reflecting the increased energy dissipation associated with cracking, damage accumulation, and frictional mechanisms in severely deteriorated masonry structures. This simplified binning strategy is adopted to provide a first-order representation of aging effects suitable for the present study, while future work will extend the framework using physically calibrated and time-dependent deterioration models.

3.3. *Fragility computation*

Collapse fragility functions are derived independently for each deterioration stage. For a given stage, the surrogate model is used to evaluate the collapse condition across all ground motion records and intensity levels. Collapse is defined as exceedance of a prescribed MIDR threshold (i.e., MIDR $\geq$ 1%), which is adopted as a simplified global collapse criterion representative of severe nonlinear damage and loss of lateral load-carrying capacity in URM structures. Although the selected threshold influences the absolute fragility estimates, the adopted value is considered adequate for the comparative evaluation of deterioration stages performed in the present study. For each intensity level, the conditional probability of collapse is computed as the fraction of simulations exceeding the collapse limit.

Then, a lognormal model is adopted to represent the collapse fragility function, expressed in terms of the selected IM. The median and dispersion parameters of the fragility function are estimated through nonlinear regression, fitting the analytical lognormal cumulative distribution function to the empirical collapse probabilities. This procedure yields a set of deterioration-dependent fragility curves that quantify the likelihood of collapse as a function of seismic intensity.

3.4. *Probabilistic modelling of collapse GWP*

The environmental impact is quantified in terms of Global Warming Potential (GWP) associated with seismic-induced collapse. A reference environmental impact, denoted as GWP_0, is defined as the baseline embodied emissions associated with the replacement of the building's structural wall components. At a selected seismic IM, the collapse probability is obtained from the corresponding fragility function. A probabilistic consequence model is then defined as a two-outcome combination:

(i) With probability equal to the collapse probability, the total GWP is modelled as a random variable representing collapse-induced replacement emissions,

(ii) With complementary probability, no collapse occurs and the total GWP contribution is set to zero.

The collapse consequence is modelled using a lognormal distribution expressed as a ratio of GWP_0, capturing uncertainty in the extent of damage and material replacement following collapse. Monte Carlo simulation is used to propagate uncertainty and generate the cumulative distribution function of the total GWP at the selected intensity level. The resulting distribution explicitly captures both the likelihood of collapse and the variability of environmental consequences conditional on collapse.

3.5. *Estimation of CO_2 emissions*

The reference environmental impact GWP_0 is estimated based on material quantities of the structural wall system. Volume of façades and internal partition walls are converted into masses using representative material densities. Embodied carbon emissions are then computed by applying representative emission factor ranges to the calculated masses.
The estimation focuses on collapse-related replacement impacts and serves as a scaling reference for the probabilistic GWP ratios derived in the previous step. This approach enables a transparent link between structural collapse assessment and environmental impact quantification while maintaining consistency with the surrogate-based probabilistic framework.

4. Results

4.1. *Collapse fragility*

Fig. 4 presents the empirical and fitted lognormal collapse fragility curves for the four deterioration stages. A clear shift of fragility functions towards lower PGA values is observed with increasing deterioration severity, denoting a progressive increase in collapse likelihood. Overall, this trend reflects the cumulative effect of reduced stiffness, strength, and deformation capacity associated with advanced deterioration stages.
The fitted fragility functions enable the direct extraction of collapse probabilities at any target seismic intensity. In general, the probability of collapse increases markedly from Stage 1 to Stage 4, highlighting the strong sensitivity of collapse risk to deterioration state. These stage-dependent collapse probabilities constitute the probabilistic input for the subsequent environmental impact assessment in the following sub-section.

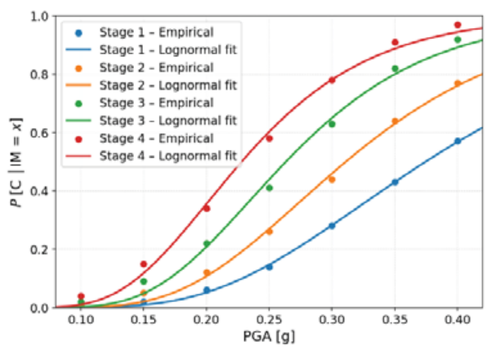

Fig. 4. Seismic collapse fragility at different aging stages.

4.2. *Probabilistic GWP*

Fig. 5 shows the cumulative distribution functions of the total GWP at PGA = 0.30 g, expressed as a percentage of a reference value GWP_0. The distributions are strictly based on collapse model observations, in which collapse results in replacement-related emissions, while non-collapse cases contribute zero GWP.

The vertical jump at GWP = 0% denotes the probability of no collapse (i.e., $1 - P[C \mid IM = x]$) for each deterioration stage, as shown in Fig. 4. As deterioration increases, this jump progressively decreases, directly reflecting the increasing likelihood of collapse inferred from the fragility analysis. Consequently, Stage 4 exhibits the smallest jump, indicating that non-collapse becomes relatively unlikely at the selected design intensity.

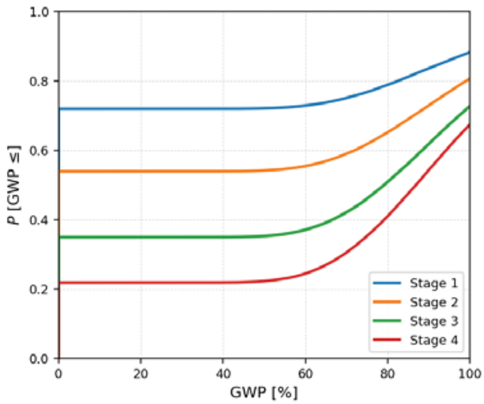

Fig. 5. Seismic collapse fragility at different aging stages.

Beyond the jump, the smooth portion of the curves represents the variability of environmental consequences conditional on collapse. Since the same collapse consequence model is assumed for all stages, differences among the curves are primarily governed by differences in collapse probability rather than by differences in collapse severity. The GWP distributions therefore provide a combined view of collapse likelihood and collapse-induced environmental impact at the design PGA.

4.3. *CO_2 emissions associated with collapse*

The reference environmental impact, GWP_0, is estimated from the embodied CO_2 emissions associated with the replacement of the building's wall system after collapse. The assessment focuses on the façade and internal partition walls, which constitute the dominant structural components in the analysed URM prototype. The total volume of façade masonry is 168.75 m³, while the volume of internal partition walls is 118.125 m³. Material densities of 1800 kg/m³ and 1200 kg/m³ are assumed for façade masonry and internal partitions, respectively, resulting in total masses of approximately 304 t and 142 t. The combined wall mass considered in the collapse scenario is therefore about 446 t.

Due to the lack of material-specific environmental data, embodied carbon emissions are estimated using representative emission-factor ranges. For façade masonry, emission factors between 0.08 and 0.25 kgCO_2e/kg are considered, while for internal partitions a range of 0.05 to 0.18 kgCO_2e/kg is assumed. These ranges, taken from the Inventory of carbon & energy (ICE) by Hammond et al. (2011), are intended to capture variability in masonry typology, binder content, and production processes. Applying these ranges yields collapse-related embodied emissions of approximately 24–76 tCO_2e for façade walls and 7–26 tCO_2e for internal partitions. The resulting total embodied emissions associated with collapse-induced wall replacement therefore range from about 31 to 101 tCO_2e, with a midpoint estimate close to 60 tCO_2e. Expressing the environmental impact in relative terms as a percentage of GWP_0 allows the probabilistic GWP curves presented in Fig. 5 to be directly interpreted in terms of absolute CO_2 emissions.

5. Summary and conclusions

An earthquake and deterioration probabilistic life-cycle assessment (EDP-LCA) methodology to assess the environmental consequences of seismic-induced collapse in deteriorated URM buildings was proposed in this study. The proposed methodology integrates nonlinear dynamic analyses, surrogate modelling, deterioration staging, fragility assessment, and life-cycle environmental impact quantification. The results highlight the strong influence of deterioration on both structural vulnerability and associated CO_2 emissions.

The collapse fragility analysis showed higher collapse probabilities with increasing deterioration severity. The probabilistic GWP assessment demonstrated that environmental consequences are governed, in this case, by collapse likelihood rather than by differences in collapse severity, which is assumed consistent across stages. For the case study building, the estimation of embodied CO_2 emissions ranges from approximately 30 to 100 tCO_2e, depending on material properties and emission-factor assumptions.

Overall, the proposed framework enables an integrated evaluation of seismic vulnerability and environmental impact for deteriorated masonry buildings, providing a consistent basis for future applications in risk-informed and sustainability-oriented seismic assessment. Future work will extend the framework to include repairable damage states below collapse, alternative building archetypes, different deterioration mechanisms, and local emission factors.

Acknowledgement
This study has been partly funded by the STAND4HERITAGE project that has received funding from the European Research Council (ERC) under the European Union's Horizon 2020 research and innovation program (Grant agreement No. 833123), as an Advanced Grant. This work was also partly financed by FCT / MCTES through national funds (PIDDAC) under the R&D Unit Institute for Sustainability and Innovation in Structural Engineering (ISISE), under reference UIDB / 04029/2020 (doi.org/10.54499/UIDB/04029/2020), and under the Associate Laboratory Advanced Production and Intelligent Systems ARISE under reference LA/P/0112/2020. This work is partly financed by national funds through FCT - Foundation for Science and Technology, under grant agreement 2023.01101.BD attributed to the first author.

References

Almeida, J. P., Beyer, K., Brunner, R. and Wenk, T., Characterization of Mortar–Timber and Timber–Timber Cyclic Friction in Timber Floor Connections of Masonry Buildings, *Materials and Structures/Materiaux et Constructions*, vol. **53**, no. 3, 2020. DOI: 10.1617/s11527-020-01483-y

Anwar, G. A., Dong, Y. and Zhai, C., Performance-Based Probabilistic Framework for Seismic Risk, Resilience, and Sustainability Assessment of Reinforced Concrete Structures, *Advances in Structural Engineering*, vol. **23**, no. 7, pp. 1454–72, 2020.

Belleri, A. and Marini, A., Does Seismic Risk Affect the Environmental Impact of Existing Buildings?, *Energy and Buildings*, vol. **110**, pp. 149–58, 2016.

Bernardo, V., Campos Costa, A., Candeias, P. and Costa, A., Seismic Vulnerability Assessment and Fragility Analysis of Pre-Code Masonry Buildings in Portugal, *Bulletin of Earthquake Engineering*, vol. **20**, no. 11, pp. 6229–65, 2022.

Caruso, M., Pinho, R., Bianchi, F., Cavalieri, F. and Lemmo, M. T., Integrated Economic and Environmental Building Classification and Optimal Seismic Vulnerability/Energy Efficiency Retrofitting, *Bulletin of Earthquake Engineering*, vol. **19**, no. 9, pp. 3627–70, 2021.

Chhabra, J. P. S., Hasik, V., Bilec, M. M. and Warn, G. P., Probabilistic Assessment of the Life-Cycle Environmental Performance and Functional Life of Buildings Due to Seismic Events, *Journal of Architectural Engineering*, vol. **24**, no. 1, p. 04017035, 2018.

Como, M., Statics of Historic Masonry Constructions: An Essay, in *Masonry Structures: Between Mechanics and Architecture*, 2015.

D'Altri, A. M., Sarhosis, V., Milani, G., Rots, J., Cattari, S., Lagomarsino, S., Sacco, E., Tralli, A., Castellazzi, G. and Miranda, S. de, Modeling Strategies for the Computational Analysis of Unreinforced Masonry Structures: Review and Classification, *Archives of Computational Methods in Engineering*, vol. **27**, no. 4, 2020. DOI: 10.1007/s11831-019-09351-x

Danciu, L., Nandan, S., Reyes, C., Basili, R., Weatherill, G., Beauval, C., Rovida, A., Vilanova, S., Şeşetyan, K. and Bard, P.-Y., The 2020 Update of the European Seismic Hazard Model: Model Overview. EFEHR Technical Report 001, v1. 0.0, 2021.

Hammond, G. and Jones, C., Embodied Carbon: The Inventory of Carbon and Energy (ICE), *BSRIA Guide University of Bath*, 2011.

Hashemi, M. J., Al-Attraqchi, A. Y., Kalfat, R. and Al-Mahaidi, R., Linking Seismic Resilience into Sustainability Assessment of Limited-Ductility RC Buildings, *Engineering Structures*, vol. **188**, pp. 121–36, 2019.

Huang, M. and Simonen, K., Comparative Environmental Analysis of Seismic Damage in Buildings, *Journal of Structural Engineering*, vol. **146**, no. 2, p. 05019002, 2020.

Li, Y., and Masera, G., Methodologies for Assessing Building Embodied Carbon in a Circular Economy Perspective, *E3S Web of Conferences*, EDP Sciences, vol. **546**, p. 01014, 2024.

McKenna, F., OpenSees: A Framework for Earthquake Engineering Simulation, *Computing in Science & Engineering*, vol. **13**, no. 4, pp. 58–66, 2011.

Nouri, A., Asadi, P. and Taheriyoun, M., Life-Cycle Cost Analysis of Seismic Designed RC Frames Including Environmental and Social Costs, *Journal of Earthquake Engineering*, vol. **26**, no. 11, pp. 5958–77, 2022.

Porter, K. A., An Overview of PEER's Performance-Based Earthquake Engineering Methodology, *9th International Conference on Applications of Statistics and Probability in Civil Engineering*, vol. **273**, no. 1995, 2003.

Simões, A. G., Bento, R., Lagomarsino, S., Cattari, S. and Lourenço, P. B., Seismic Assessment of Nineteenth and Twentieth Centuries URM Buildings in Lisbon: Structural Features and Derivation of Fragility Curves, *Bulletin of Earthquake Engineering*, vol. **18**, no. 2, pp. 645–72, 2020.

Simões, A., Evaluation of the Seismic Vulnerability of the Unreinforced Masonry Buildings Constructed in the Transition between the 19th and 20th Centuries in Lisbon, Portugal, *Instituto Superior Técnico, Lisboa*, 2018.

Stein, M., Large Sample Properties of Simulations Using Latin Hypercube Sampling, *Technometrics*, vol. **29**, no. 2, 1987. DOI: 10.1080/00401706.1987.10488205

Tomić, I., Vanin, F. and Beyer, K., Uncertainties in the Seismic Assessment of Historical Masonry Buildings, *Applied Sciences (Switzerland)*, vol. **11**, no. 5, 2021. DOI: 10.3390/app11052280

Vamvatsikos, D. and Cornell, C. A., Incremental Dynamic Analysis, *Earthquake Engineering & Structural Dynamics*, vol. **31**, no. 3, pp. 491–514, 2002.

Vanin, F., Penna, A. and Beyer, K., A Three-Dimensional Macroelement for Modelling the in-Plane and out-of-Plane Response of Masonry Walls, *Earthquake Engineering and Structural Dynamics*, vol. **49**, no. 14, 2020a. DOI: 10.1002/eqe.3277

Vanin, F., Penna, A. and Beyer, K., Equivalent-Frame Modeling of Two Shaking Table Tests of Masonry Buildings Accounting for Their Out-Of-Plane Response, *Frontiers in Built Environment*, vol. **6**, 2020b. DOI: 10.3389/fbuil.2020.00042

Vanin, F., Zaganelli, D., Penna, A. and Beyer, K., Estimates for the Stiffness, Strength and Drift Capacity of Stone Masonry Walls Based on 123 Quasi-Static Cyclic Tests Reported in the Literature, *Bulletin of Earthquake Engineering*, vol. **15**, no. 12, 2017. DOI: 10.1007/s10518-017-0188-5

Wei, H.-H., Shohet, I. M., Skibniewski, M. J., Shapira, S. and Yao, X., Assessing the Lifecycle Sustainability Costs and Benefits of Seismic Mitigation Designs for Buildings, *Journal of Architectural Engineering*, vol. **22**, no. 1, p. 04015011, 2016.

Welsh-Huggins, S. J., Liel, A. B. and Cook, S. M., Reduce, Reuse, Resilient? Life-Cycle Seismic and Environmental Performance of Buildings with Alternative Concretes, *Journal of Infrastructure Systems*, vol. **26**, no. 1, p. 04019033, 2020.